

This is the accepted manuscript made available via CHORUS. The article has been published as:

Superconductivity, pairing symmetry, and disorder in the doped topological insulator $\text{Sn}_{1-x}\text{In}_x\text{Te}$ for $x \geq 0.10$

M. P. Smylie, H. Claus, W.-K. Kwok, E. R. Louden, M. R. Eskildsen, A. S. Sefat, R. D. Zhong, J. Schneeloch, G. D. Gu, E. Bokari, P. M. Niraula, A. Kayani, C. D. Dewhurst, A. Snezhko, and U. Welp

Phys. Rev. B **97**, 024511 — Published 19 January 2018

DOI: [10.1103/PhysRevB.97.024511](https://doi.org/10.1103/PhysRevB.97.024511)

Superconductivity, pairing symmetry, and disorder in the doped topological insulator $\text{Sn}_{1-x}\text{In}_x\text{Te}$ for $x \geq 0.10$

M. P. Smylie,^{1,2} H. Claus,¹ W.-K. Kwok,¹ E. R. Loudon,² M. R. Eskildsen,² A. S. Sefat,³ R. D. Zhong,^{4,5} J. Schneeloch,^{4,6} G. D. Gu,⁴ E. Bokari,⁷ P. M. Niraula,⁷ A. Kayani,⁷ C. D. Dewhurst,⁸ A. Snezhko,¹ and U. Welp¹

¹*Materials Science Division, Argonne National Laboratory, 9700 S. Cass Ave., Argonne, Illinois 60439*

²*Department of Physics, University of Notre Dame, Notre Dame, Indiana 46556*

³*Materials Science and Technology Division, Oak Ridge National Laboratory, Oak Ridge, Tennessee 37831*

⁴*Condensed Matter Physics and Materials Science Department,
Brookhaven National Laboratory, Upton, New York 11973*

⁵*Materials Science and Engineering Department,
Stony Brook University, Stony Brook, New York 11749*

⁶*Department of Physics and Astronomy, Stony Brook University, Stony Brook, New York 11973*

⁷*Department of Physics, Western Michigan University, Kalamazoo, Michigan 49008*

⁸*Institut Laue-Langevin, 6 Rue Jules Horowitz, F-38042 Grenoble, France*

The temperature dependence of the London penetration depth $\Delta\lambda(T)$ in the superconducting doped topological crystalline insulator $\text{Sn}_{1-x}\text{In}_x\text{Te}$ was measured down to 450 mK for two different doping levels, $x \approx 0.45$ (optimally doped) and $x \approx 0.10$ (underdoped), bookending the range of cubic phase in the compound. The results indicate no deviation from fully gapped BCS-like behavior, eliminating several candidate unconventional gap structures. Critical field values below 1 K and other superconducting parameters are also presented. The introduction of disorder by repeated particle irradiation with 5 MeV protons does not enhance T_c , indicating that ferroelectric interactions do not compete with superconductivity.

I. INTRODUCTION

Recently, there has been significant attention given to topological states in solids, particularly towards topological insulators (TI)^{1,2} and topological superconductors (TSC)^{3,4}, because of the properties of their novel quantum states. A topological insulator is a material that is insulating in the bulk, but has gapless surface states that conduct; these states are protected by time-reversal symmetry in the material. In topological crystalline insulators (TCIs)⁵, the gapless surface state is instead protected by the mirror symmetry of the crystal. Following confirmation of Bi_2Se_3 , Bi_2Te_3 , and Sb_2Te_3 as topological insulators, a few materials have been identified as topological crystalline insulators⁶ including $\text{Pb}_{1-x}\text{Sn}_x\text{Se}$, $\text{Pb}_{1-x}\text{Sn}_x\text{Te}$, and SnTe ^{7,8}. Topological superconductors support gapless surface quasiparticle states that can host Majorana fermions, whose non-Abelian statistics may form the basis for new approaches to fault-tolerant quantum computing^{9–12}. Two routes are currently being pursued^{3,4,6,13} to create a topological superconductor: proximity induced at the interface between strong spin-orbit coupling semiconductors and conventional superconductors, or by chemical doping of bulk TI and TCI materials. Among the latter, the first materials suggested to be bulk topological superconductors were obtained by doping Bi_2Se_3 : $\text{Cu}_x\text{Bi}_2\text{Se}_3$ ^{14–18} with $T_c \sim 3.5$ K, $\text{Nb}_x\text{Bi}_2\text{Se}_3$ with $T_c \sim 3.4$ K and $\text{Sr}_x\text{Bi}_2\text{Se}_3$ ^{19–23} with $T_c \sim 3.0$ K. More recently, surface Andreev bound states in In-doped SnTe crystals have been observed²⁴ via point-contact spectroscopy; the presence of such zero-bias conductivity peaks are generally interpreted as sign of unconventional superconductivity²⁵. Thermal conductivity measurements²⁶ on a $\text{Sn}_{0.6}\text{In}_{0.4}\text{Te}$ crystal suggest

a full gap, and Knight shift measurements²⁷ on a polycrystalline sample with $\sim 4\%$ doping may indicate a spin-singlet state. In systems with time reversal and inversion symmetry, odd-parity pairing is a requirement for topological superconductivity. Thus, determining the superconducting gap structure is important to establishing the possibility of topological superconductivity, as not all theoretically allowed²⁴ gap structures are unconventional, odd-parity states.

The phase diagram of $\text{Sn}_{1-x}\text{In}_x\text{Te}$ is known to contain several phases²⁸. The parent compound SnTe undergoes a ferroelectric transition at up to 100 K; this transition temperature decreases to zero with increasing hole concentration²⁹. The ferroelectric transition is accompanied by a structural phase change from cubic to rhombohedral. At sub-Kelvin temperatures, the parent material becomes superconducting^{30,31}. It was discovered that In-doping on the Sn site increases the superconducting transition temperature by an order of magnitude, a surprising result considering its low carrier density of $\sim 10^{21} \text{ cm}^{-3}$. More recent efforts^{32,33}, spurred by the growing interest in topological materials, have raised the transition temperature in $\text{Sn}_{1-x}\text{In}_x\text{Te}$ to 4.5 K with better synthesis techniques. The low-temperature phase diagram is separated into two crystal structures: for $x < 0.04$, the structure is rhombohedral, and for $x > 0.04$, the structure is face centered cubic. For a narrow range of doping ($0.02 < x < 0.04$), the compound $\text{Sn}_{1-x}\text{In}_x\text{Te}$ is both ferroelectric and superconducting, both of which are thought to be bulk in nature. In this range, T_c is below 2 K and is not a function of x ²⁸. Above this range, up to the solubility limit of $x \sim 0.45$, T_c increases linearly with x to a maximum of ~ 4.5 K. Recent reports suggest^{28,34} that the pairing mechanism may be different

for low and high doping levels, and that disorder scattering may have a strong effect on the transition temperature. In as-grown crystals shown to have equal carrier concentrations²⁸, crystals with higher normal-state resistivity systematically have higher T_c 's. This may be due to either disorder favoring even pairing channels over odd^{35,36} or by favoring superconducting over ferroelectric interactions.

In this work, we report on magnetization measurements and low-temperature measurements of the London penetration depth λ . The temperature dependence of λ indicates a full superconducting gap. Increased electron scattering induced by particle irradiation does not enhance T_c in the cubic phase of $\text{Sn}_{1-x}\text{In}_x\text{Te}$ implying that for higher doping levels, the competition between ferroelectric, odd-parity, and even parity is weak if extant, as odd-parity pairing is conventionally thought to be very sensitive to nonmagnetic disorder³⁷.

II. EXPERIMENTAL METHODS

Crystals of $\text{Sn}_{0.9}\text{In}_{0.1}\text{Te}$ and $\text{Sn}_{0.55}\text{In}_{0.45}\text{Te}$ were grown by the modified Bridgman method, following the work of Tanaka³⁸. This range of x was chosen to cover the range of the cubic superconducting phase while remaining clearly above the cubic-rhombohedral structural transition. X-ray diffraction and EDS measurements were used to verify the crystal structure and stoichiometry.

Magnetometry measurements were performed both with a Quantum Design MPMS dc SQUID magnetometer with a superconducting magnet down to 1.8 K, and a custom-built SQUID magnetometer with a conventional magnet down to 1.2 K. The tunnel diode oscillator (TDO) technique^{39,40} was used to measure the temperature dependence of the London penetration depth $\Delta\lambda(T) = \lambda(T) - \lambda_0$ with λ_0 the zero-temperature value in various applied magnetic fields down to 400 mK in a ^3He cryostat with a custom^{20,41,42} resonator operating at ~ 14.5 MHz. To image the vortex lattice in the superconducting state and to obtain an independent estimate of λ_0 , complementary small-angle neutron scattering (SANS) measurements were performed at 50 mK on the D33 beam line at the Institut Laue-Langevin in Grenoble, France⁴³. To examine the role of disorder, repeated irradiation with 5-MeV protons was performed at the tandem Van de Graaf accelerator at Western Michigan University. Irradiation with MeV-energy protons creates a distribution of defects, ranging from Frenkel pairs of point defects to collision cascades and clusters^{44–46}, all of which enhance electron scattering. During irradiation the samples were cooled to approximately -10 °C to prevent local heating of the sample. Samples selected for irradiation were ~ 55 μm thick, and TRIM simulations show that the defect generation at 5-MeV is essentially uniform across such a thickness.

III. RESULTS AND DISCUSSION

X-ray diffraction measurements verifying the crystal structure and purity are shown in Fig. 1. At both doping

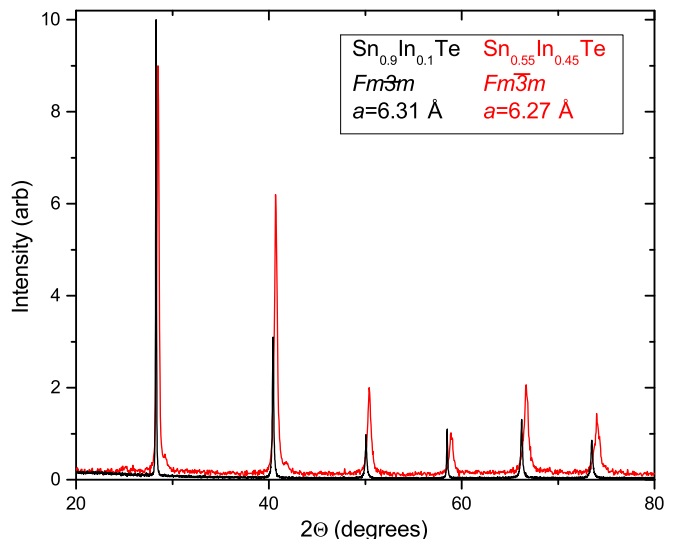


FIG. 1: Diffraction data verifying single-phase FCC structure in underdoped and optimally doped $\text{Sn}_{1-x}\text{In}_x\text{Te}$. In both materials, the lattice constants are consistent with the doping levels as measured through EDS analysis.

levels, the material is single phase with rocksalt structure (space group $Fm\bar{3}m$), with lattice parameters $a = 6.31$ Å for $x \approx 0.1$, and $a = 6.27$ Å for $x \approx 0.45$. Through EDS analysis the composition was determined, yielding values close to the nominal stoichiometry.

Estimates of λ_0 can be obtained from measurements of the lower critical field H_{c1} and upper critical field H_{c2} . Values of H_{c1} for both doping levels were deduced from low-temperature magnetization measurements shown in Fig. 2. For the optimally doped material, magnetization measurements versus applied field [Fig. 2(a)] were used; for the $x \approx 0.1$ material, magnetization versus temperature measurements at multiple fixed fields in the range of 0.1-1.8 G [Fig. 2(b)] were performed, and magnetization versus applied field could be extracted from isothermal data. In both cases, the penetration field H_p ^{41,47} was taken as the field for which the magnetization deviates away from being linear in H . Using the Brandt formulation⁴⁷, we calculate the corrections due to edge and/or surface barriers to vortex penetration yielding estimates of H_{c1} as shown in Fig. 4. For a platelike superconductor, $H_p/H_{c1} = \tanh\left(\sqrt{\alpha t/w}\right)$, where t and w are the thickness and width, and $\alpha = 0.67$ for a disc-shaped sample. Upper and lower critical field data for both doping levels are shown in Fig. 4. With a conventional parabolic temperature dependence $H_{c1} = H_{c1}(0) (1 - (T/T_c)^2)$ we extrapolate $H_{c1} = 7.96$ G and 32.0 G as the zero-temperature values for $x \approx 0.1$ and $x \approx 0.45$, respectively.

The TDO frequency shift is proportional to the magnetic susceptibility^{39,40} of the sample, allowing for the detection of the superconducting transition as shown in Fig. 3 for field values up to 2 T for small crystals of both doping levels. No secondary superconducting tran-

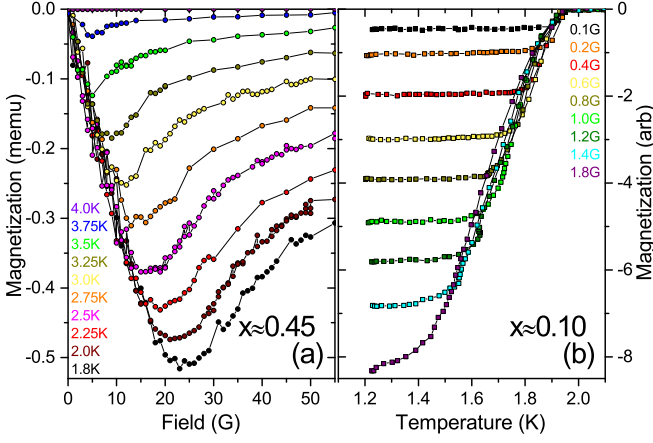


FIG. 2: (a) Magnetization versus applied magnetic field sweeps on optimally doped $\text{Sn}_{1-x}\text{In}_x\text{Te}$ at various temperatures from 1.8 K through 4.0 K, measured in a conventional MPMS SQUID. (b) Magnetization versus temperature sweeps on 10% doped $\text{Sn}_{1-x}\text{In}_x\text{Te}$ at various fields from 0.1 G to 1.8 G, measured in a custom dc SQUID. Isothermal magnetization versus field curves are extracted from this data. In both datasets, H_p is determined as the field for which the magnetization deviates away from being linear in H .

sitions were observable in either sample up to 20 K. Defining the onset T_c to be at the deviation in slope of the TDO frequency shift from the essentially temperature independent value at temperatures above T_{c0} yields the $H_{c2}(T)$ data shown in Fig. 4. The phenomenological relation $H_{c2}(T) = H_{c2}(0) \left(\frac{1-t^2}{1+t^2} \right)$, shown in red in Fig. 4, describes the data well, as has been observed for other superconducting doped topological insulators⁴⁸. This yields a zero-temperature limit of the upper critical field H_{c2} of approximately 1.04 T for the underdoped sample, and for the near-optimally doped sample, $H_{c2}(0) \approx 1.94$ T. Both values are well below the BCS Pauli paramagnetic limit of $B_{c2}^{\text{Pauli}} = 1.83T_c$. From our values of H_{c2} , we calculate the coherence length ξ_0 for both doping levels using the Ginzburg-Landau relation $\mu_0 H_{c2}(0) = \Phi_0 / 2\pi \xi^2(0)$, resulting in $\xi_0 = 17.8$ nm for $x \approx 0.1$ and $\xi_0 = 13.0$ nm for $x \approx 0.45$. With the extrapolated zero-temperature H_{c2} values and using the Ginzburg-Landau formula $H_{c1} = \Phi_0 / (4\pi \lambda^2) (\ln[\lambda/\xi] + 0.5)$, we determine estimates for the zero-temperature value of λ to be 900 nm for $x \approx 0.1$ and 425 nm for $x \approx 0.45$; such large values are consistent with values from NMR²⁷ (~ 1200 nm, $x = 0.04$) and μSR ⁴⁹ (542 nm, $x = 0.4$).

SANS measurements were performed on oriented crystals of $\text{Sn}_{0.9}\text{In}_{0.1}\text{Te}$. Data was collected at 50 mK for applied magnetic fields ranging from 0.1 to 0.3 T directed along various high symmetry directions, but no vortex lattice could be detected. From the background intensity, a lower limit of the London penetration depth λ_0 may be extracted from the neutron reflectivity R :

$$R = \frac{2\pi\gamma_n^2 t \gamma^2}{16\phi_0^2 q} \frac{B^2}{(1 + \lambda^2 q^2)^2} \exp(-2c\xi^2 q^2) \quad (1)$$

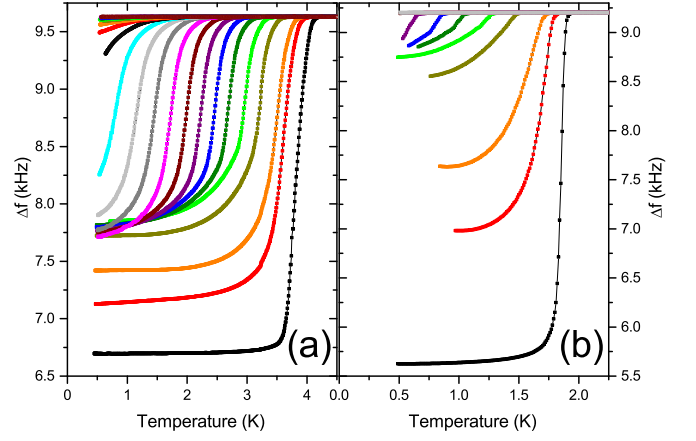


FIG. 3: TDO measurements showing suppression of superconductivity in applied magnetic fields up to 2.1 T for near-optimally doped (a) and underdoped (b) $\text{Sn}_{1-x}\text{In}_x\text{Te}$.

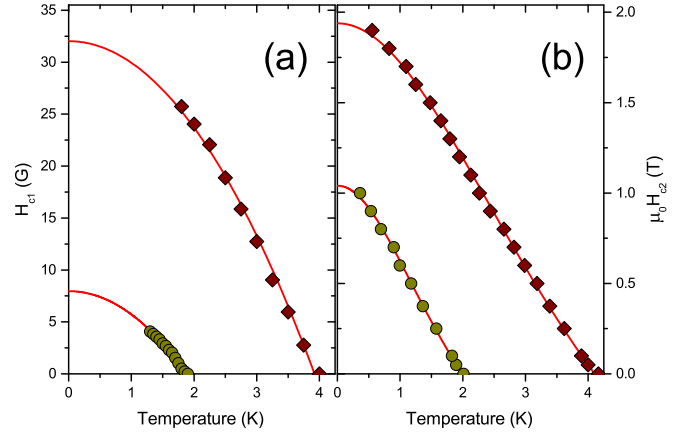


FIG. 4: Critical field H_{c1} (a) and H_{c2} (b) values for underdoped (yellow circles) and near-optimal (red diamonds) $\text{Sn}_{1-x}\text{In}_x\text{Te}$. Extrapolated zero-temperature values for H_{c1} are 7.92 G and 32.0 G, and for H_{c2} 1.04 T and 1.94 T, for underdoped and near-optimal, respectively.

where γ_n is neutron gyromagnetic ratio, t the sample thickness, B the applied magnetic field, $\phi_0 = 2067$ T nm² the flux quantum, q the scattering vector, and ξ the coherence length, with c a constant typically taken as 0.5⁵⁰. Our SANS results put a lower limit of 550 nm on λ_0 , consistent with our direct estimate of λ_0 via lower and upper critical fields.

Low temperature penetration depth measurements were carried out via the TDO technique in the temperature range from 0.4 to 40 K. In the TDO technique, the frequency shift δf of the resonator is proportional to the change of the penetration depth⁴⁰:

$$\delta f(T) = G\Delta\lambda(T) \quad (2)$$

where the geometrical factor G depends on the sample shape and volume as well as the geometry of the resonator coil. The magnetic field of the resonator coil is ~ 20 mOe,

assuring that the sample remains fully in the Meissner state.

The low-temperature variation of the London penetration depth $\Delta\lambda(T) = \lambda(T) - \lambda_0$ can provide information on the superconducting gap structure³⁹. In the low temperature limit, conventional BCS theory for an isotropic *s*-wave superconductor yields an exponential variation of $\Delta\lambda(T)$:

$$\frac{\Delta\lambda(T)}{\lambda_0} \approx \sqrt{\frac{\pi\Delta_0}{2T}} \exp\left(\frac{-\Delta_0}{T}\right) \quad (3)$$

with λ_0 and Δ_0 the zero-temperature values of the penetration depth and energy gap. In contrast, in nodal superconductors the enhanced thermal excitation of quasiparticles near the gap nodes results in a power law variation, $\Delta\lambda \sim T^n$ ^{20,39,51} where the exponent n depends on the nature of the nodes and the degree of electron scattering.

The evolution of the low temperature TDO response of a single crystal of $\text{Sn}_{0.55}\text{In}_{0.45}\text{Te}$ is shown in Fig. 5. The inset shows the full transition, which is very sharp, indicating a high quality material. The behavior of the optimally doped material can be well described by an exponential dependence with a BCS-like gap value (red line) below $T_c/3$, indicating that the material is a fully-gapped superconductor, in agreement with thermal conductivity and muon-spin spectroscopy measurements^{26,49}. Our data extend a recent report⁵² to low temperatures where Eq. 3 is actually applicable. The low gap ratio of $\Delta_0/T_c = 1.18$ is not consistent with standard BCS *s*-wave theory which predicts $\Delta_0/T_c = 1.76$, but is consistent with a weakly anisotropic single gap^{53–55} as the temperature dependence of λ probes quasiparticle excitations at the lowest activation energy.

The $x \approx 0.1$ doping level is slightly above the value separating the ferroelectric rhombohedral phase and the cubic phase. The low temperature TDO response for a single crystal of $\text{Sn}_{0.9}\text{In}_{0.1}\text{Te}$ is shown in Fig. 6. The inset shows the full transition, which is very sharp. As T_c is low we do not reach very far below the low temperature limit of $T_c/3$; nevertheless, in the accessible temperature range the data are well described by a BCS-like exponential fit (red). A gap ratio of $\Delta_0/T_c = 1.76$ provides an excellent fit to the data, suggesting a full, isotropic BCS-like superconducting gap.

Recent theoretical studies^{24,56} show that only three pairing symmetries are possible that do not spontaneously break any lattice symmetry, namely the A_{1g} , A_{1u} , and A_{2u} representations of D_{3d} . A_{1g} is even parity and fully gapped and corresponds to the *s*-wave state that does not allow topological behavior. A_{1u} is odd parity and fully gapped; A_{2u} is odd parity and has symmetry-protected point nodes. Our TDO measurements exclude the A_{2u} parity and point to one of the two fully-gapped states. If there is unconventional superconductivity in $\text{Sn}_{1-x}\text{In}_x\text{Te}$, it must be the A_{1u} state, consistent with band structure arguments²⁴ that suggest that the pairing symmetry has odd parity. Recent Knight shift

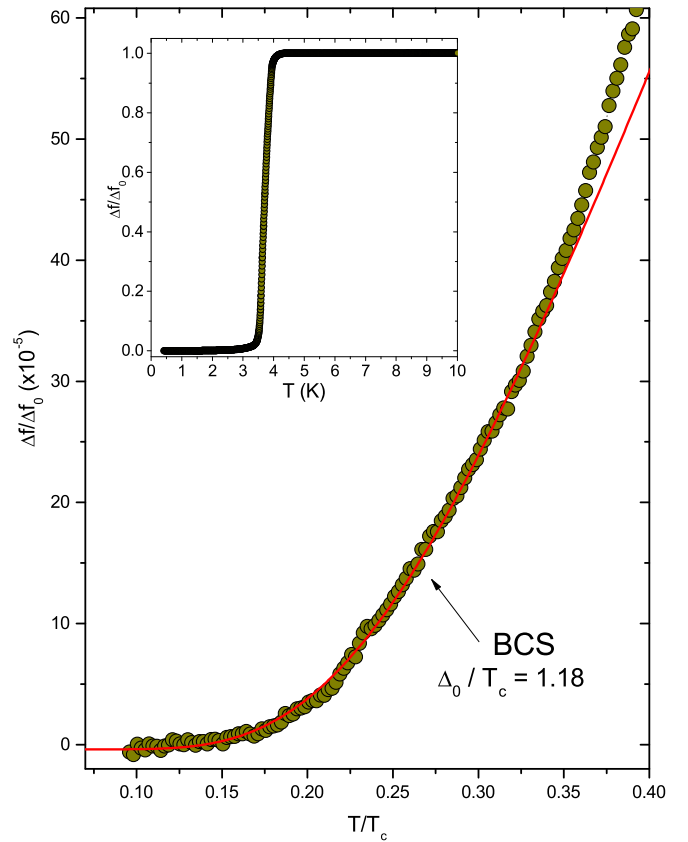


FIG. 5: Normalized low temperature frequency shift $\Delta f(T)$ for $\text{Sn}_{0.55}\text{In}_{0.45}\text{Te}$. The BCS-like fit (red) well describes the data. The inset shows the full, sharp transition, with no evidence of other low-temperature phases.

measurements²⁷ on a polycrystalline sample with 4% In-doping yielded an incomplete suppression of the Knight shift that was nevertheless larger than the expected value for spin-triplet pairing. These results were interpreted as signature of spin-singlet behavior. However, since the doping level of this sample is right at the cubic-rhombohedral transition, further studies on higher-doped single-crystals may be needed to obtain a definite answer. More exotic pairing symmetries would be allowed if evidence of rotational symmetry breaking is seen, as is the case in the doped Bi_2Se_3 family of superconductors^{57–59}.

An open question relates to the effect of disorder scattering in $\text{Sn}_{1-x}\text{In}_x\text{Te}$. TDO and SQUID magnetometry measurements following repeated irradiations with 5 MeV protons up to a high total dose of 2×10^{17} p/cm² on three crystals of $\text{Sn}_{1-x}\text{In}_x\text{Te}$ with different doping levels are shown in Fig. 7. There is essentially no or only very small change in the transition temperature upon p-irradiation. On a thin $\text{Sn}_{0.55}\text{In}_{0.45}\text{Te}$ crystal we observed a $\sim 67\%$ increase of the normal state resistivity following p-irradiation to a dose of 5×10^{16} p/cm². However, degradation of the electrical contacts prevented repeated irradiations. The results in Fig. 7 would be in agreement with expectations based on Anderson's theorem⁶⁰

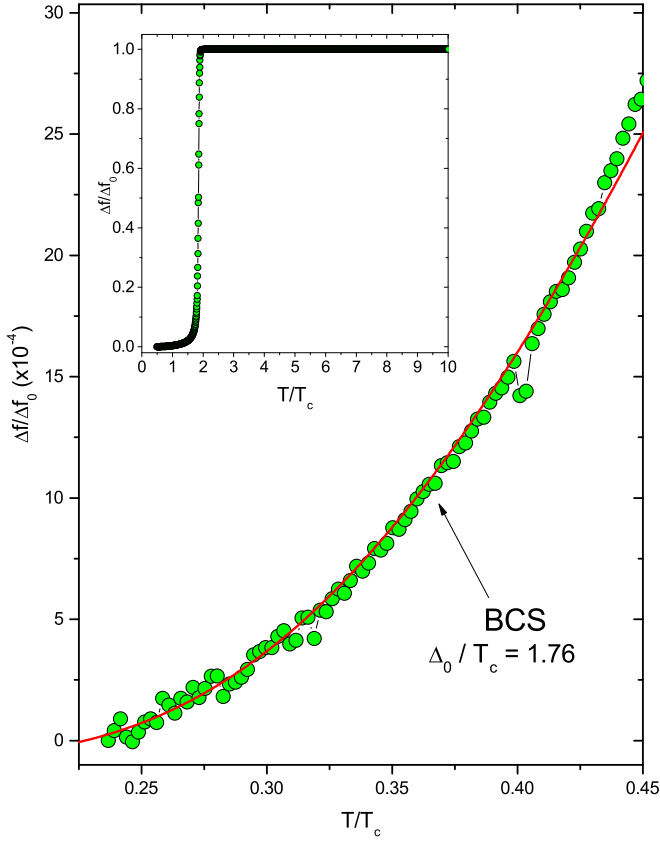


FIG. 6: Normalized low temperature frequency shift $\Delta f(T)$ for $\text{Sn}_{0.9}\text{In}_{0.1}\text{Te}$. The BCS-like fit (red) well describes the data. The inset shows the full, sharp transition, with no evidence of other low-temperature phases.

which states that T_c of an isotropic s -wave superconductor should be unaffected by non-magnetic potential scattering. However, recently it has been recognized that due to strong spin-orbit coupling effects, T_c in topological superconductors is surprisingly insensitive to non-magnetic scattering^{61–63} regardless of the superconducting gap structure. Thus, the results presented here are consistent with either A_{1g} or A_{1u} gap symmetry.

In an earlier study it was observed²⁸ that for $\text{Sn}_{1-x}\text{In}_x\text{Te}$ crystals with low In-doping, T_c is higher for samples with higher resistivity. Within conventional Abrikosov-Gorkov theory⁶⁴ and extensions thereof⁶⁵, increased electron scattering due to static non-magnetic disorder is not expected to enhance T_c . Recently, it has been proposed⁶⁶ that phonon coupling at non-magnetic Anderson- U impurities may enhance T_c . Alternatively, an increase of T_c may also occur when competing orders coexist and enhanced electron scattering affects the competing order more than it affects superconductivity. Such a situation may arise in the charge density wave materials 2H-TaSe₂ and 2H-TaS₂ where electron irradiation causes an increase of T_c ⁶⁷. In our case, $\text{Sn}_{1-x}\text{In}_x\text{Te}$ at low values of x is rhombohedral and displays ferroelectric and superconducting order. Thus, the increase of T_c

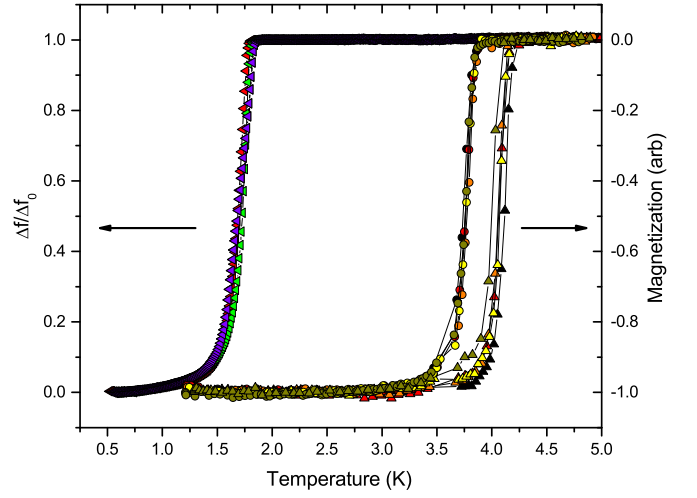


FIG. 7: Superconducting transitions following repeated irradiations with 5 MeV protons in a crystal of underdoped $\text{Sn}_{0.9}\text{In}_{0.1}\text{Te}$ ($T_c = 1.8$ K) and two crystals of near-optimally doped $\text{Sn}_{0.55}\text{In}_{0.45}\text{Te}$ ($T_c = 3.8$ K, 4.1 K) as measured by TDO and SQUID magnetometry, respectively. With doses up to 2×10^{17} p/cm², there is essentially no change in the transition temperature.

with increased electron scattering as reported in Ref. 28 for low-doped samples may have a similar cause as proposed for TaSe₂ and TaS₂. The authors of Ref. 28 point out that the correlation between disorder and T_c is much weaker in the higher doped cubic, purely superconducting phase. Our samples presented in Fig. 7 are in this phase. At this point no structural studies are available that would identify the nature of the disorder giving rise to the enhanced resistivity in the low-doped samples or the nature of the p-irradiation induced defects.

IV. CONCLUSION

In summary, we have investigated the superconducting properties of the topological crystalline insulator-derived superconductor $\text{Sn}_{1-x}\text{In}_x\text{Te}$, and have shown it to be a fully-gapped superconductor for $x \geq 0.10$ with anisotropy increasing with doping. Magnetic phase diagrams have been extended to < 1 K. One of the two suggested types of odd-parity pairings (A_{2u}) cannot describe this material as our results rule out nodal behavior, and the reports of unconventional superconductivity in the material are thus only consistent with the A_{1u} pairing, making $\text{Sn}_{1-x}\text{In}_x\text{Te}$ a strong candidate for a topological superconductor. Proton irradiation does not enhance T_c at any studied doping level, indicating that increasing scattering does not enhance T_c by destroying possible competing ferroelectric interactions or odd parity pairing in the cubic phase. To fully investigate the interplay of ferroelectricity and superconductivity (and the possibility of competition between odd-parity vs even parity superconductivity), further studies on samples with lower doping will be necessary.

ACKNOWLEDGMENTS

TDO and magnetization measurements were supported by the U.S. Department of Energy, Office of Science, Basic Energy Sciences, Materials Sciences and Engineering Division. SANS measurements were supported by the U.S. Department of Energy, Office of Basic Energy Sciences, under Award No. DE-SC0005051. M.P.S. thanks ND Energy for supporting his research and professional development through the ND Energy Postdoctoral Fellowship Program. Work at Brookhaven was sup-

ported by the Office of Basic Energy Sciences (BES), Division of Materials Science and Engineering, U.S. Department of Energy (DOE), through Contract No. DE-SC0012704. R. D. Z. and J. S. were supported by the Center for Emergent Superconductivity, an Energy Frontier Research Center funded by BES. The work at ORNL was supported by the US Department of Energy, Basic Energy Sciences, Materials Sciences and Engineering Division. We acknowledge that crystal growth was enabled by individuals such as of M. Susner.

- ¹ M. Z. Hasan and C. L. Kane, *Rev. Mod. Phys.* **82**, 3045 (2010), URL <https://link.aps.org/doi/10.1103/RevModPhys.82.3045>.
- ² Y. Ando, *Journal of the Physical Society of Japan* **82**, 102001 (2013), <https://doi.org/10.7566/JPSJ.82.102001>, URL <https://doi.org/10.7566/JPSJ.82.102001>.
- ³ X.-L. Qi and S.-C. Zhang, *Rev. Mod. Phys.* **83**, 1057 (2011), URL <https://link.aps.org/doi/10.1103/RevModPhys.83.1057>.
- ⁴ S. Sasaki and T. Mizushima, *Superconducting Materials: Conventional, Unconventional and Undetermined* **514**, 206 (2015), ISSN 0921-4534, URL <http://www.sciencedirect.com/science/article/pii/S0921453415000453>.
- ⁵ L. Fu, *Phys. Rev. Lett.* **106**, 106802 (2011), URL <https://link.aps.org/doi/10.1103/PhysRevLett.106.106802>.
- ⁶ Y. Ando and L. Fu, *Annual Review of Condensed Matter Physics* **6**, 361 (2015), <https://doi.org/10.1146/annurev-conmatphys-031214-014501>, URL <https://doi.org/10.1146/annurev-conmatphys-031214-014501>.
- ⁷ T. H. Hsieh, H. Lin, J. Liu, W. Duan, A. Bansil, and L. Fu, *Nature Communications* **3**, 982 (2012), URL <http://dx.doi.org/10.1038/ncomms1969>.
- ⁸ T. Sato, Y. Tanaka, K. Nakayama, S. Souma, T. Takahashi, S. Sasaki, Z. Ren, A. A. Taskin, K. Segawa, and Y. Ando, *Phys. Rev. Lett.* **110**, 206804 (2013), URL <https://link.aps.org/doi/10.1103/PhysRevLett.110.206804>.
- ⁹ F. Wilczek, *Nat. Phys.* **5**, 614 (2009), ISSN 1745-2473, URL <http://dx.doi.org/10.1038/nphys1380>.
- ¹⁰ C. W. J. Beenakker, *Annu. Rev. Condens. Matter Phys.* **4**, 113 (2013), ISSN 1947-5454, URL <https://doi.org/10.1146/annurev-conmatphys-030212-184337>.
- ¹¹ S. M. Albrecht, A. P. Higginbotham, M. Madsen, F. Kuemmeth, T. S. Jespersen, J. Nygrd, P. Krogstrup, and C. M. Marcus, *Nature* **531**, 206 (2016), URL <http://dx.doi.org/10.1038/nature17162>.
- ¹² V. Mourik, K. Zuo, S. M. Frolov, S. R. Plissard, E. P. A. M. Bakkers, and L. P. Kouwenhoven, *Science* **336**, 1003 (2012), URL <http://science.sciencemag.org/content/336/6084/1003.abstract>.
- ¹³ M. Sato and Y. Ando, *Reports on Progress in Physics* **80**, 076501 (2017), ISSN 0034-4885, URL <http://stacks.iop.org/0034-4885/80/i=7/a=076501>.
- ¹⁴ Y. S. Hor, A. J. Williams, J. G. Checkelsky, P. Roushan, J. Seo, Q. Xu, H. W. Zandbergen, A. Yazdani, N. P. Ong, and R. J. Cava, *Phys. Rev. Lett.* **104**, 057001 (2010), URL <https://link.aps.org/doi/10.1103/PhysRevLett.104.057001>.
- ¹⁵ P. Das, Y. Suzuki, M. Tachiki, and K. Kadowaki, *Phys. Rev. B* **83**, 220513 (2011), URL <https://link.aps.org/doi/10.1103/PhysRevB.83.220513>.
- ¹⁶ M. Kriener, K. Segawa, Z. Ren, S. Sasaki, and Y. Ando, *Phys. Rev. Lett.* **106**, 127004 (2011), URL <https://link.aps.org/doi/10.1103/PhysRevLett.106.127004>.
- ¹⁷ M. Kriener, K. Segawa, Z. Ren, S. Sasaki, S. Wada, S. Kuwabata, and Y. Ando, *Phys. Rev. B* **84**, 054513 (2011), URL <https://link.aps.org/doi/10.1103/PhysRevB.84.054513>.
- ¹⁸ J. A. Schneeloch, R. D. Zhong, Z. J. Xu, G. D. Gu, and J. M. Tranquada, *Phys. Rev. B* **91**, 144506 (2015), URL <https://link.aps.org/doi/10.1103/PhysRevB.91.144506>.
- ¹⁹ Y. Qiu, K. Nocon Sanders, J. Dai, J. E. Medvedeva, W. Wu, P. Ghaemi, T. Vojta, and Y. San Hor, *ArXiv e-prints* (2015), 1512.03519.
- ²⁰ M. P. Smylie, H. Claus, U. Welp, W.-K. Kwok, Y. Qiu, Y. S. Hor, and A. Snezhko, *Phys. Rev. B* **94**, 180510 (2016), URL <https://link.aps.org/doi/10.1103/PhysRevB.94.180510>.
- ²¹ Z. Liu, X. Yao, J. Shao, M. Zuo, L. Pi, S. Tan, C. Zhang, and Y. Zhang, *J. Am. Chem. Soc.* **137**, 10512 (2015), ISSN 0002-7863, URL <http://dx.doi.org/10.1021/jacs.5b06815>.
- ²² Shruti, V. K. Maurya, P. Neha, P. Srivastava, and S. Patnaik, *Phys. Rev. B* **92**, 020506 (2015), URL <https://link.aps.org/doi/10.1103/PhysRevB.92.020506>.
- ²³ Z. Wang, A. A. Taskin, T. Frlich, M. Braden, and Y. Ando, *Chem. Mater.* **28**, 779 (2016), ISSN 0897-4756, URL <http://dx.doi.org/10.1021/acs.chemmater.5b03727>.
- ²⁴ S. Sasaki, Z. Ren, A. A. Taskin, K. Segawa, L. Fu, and Y. Ando, *Phys. Rev. Lett.* **109**, 217004 (2012), URL <https://link.aps.org/doi/10.1103/PhysRevLett.109.217004>.
- ²⁵ S. Kashiwaya and Y. Tanaka, *Reports on Progress in Physics* **63**, 1641 (2000), ISSN 0034-4885, URL <http://stacks.iop.org/0034-4885/63/i=10/a=202>.
- ²⁶ L. P. He, Z. Zhang, J. Pan, X. C. Hong, S. Y. Zhou, and S. Y. Li, *Phys. Rev. B* **88**, 014523 (2013), URL <https://link.aps.org/doi/10.1103/PhysRevB.88.014523>.
- ²⁷ S. Maeda, R. Hirose, K. Matano, M. Novak, Y. Ando, and G.-q. Zheng, *Phys. Rev. B* **96**, 104502 (2017), URL <https://link.aps.org/doi/10.1103/PhysRevB.96.104502>.
- ²⁸ M. Novak, S. Sasaki, M. Kriener, K. Segawa, and Y. Ando, *Phys. Rev. B* **88**, 140502 (2013), URL <https://link.aps.org/doi/10.1103/PhysRevB.88.140502>.

- ²⁹ A. S. Erickson, J.-H. Chu, M. F. Toney, T. H. Geballe, and I. R. Fisher, *Phys. Rev. B* **79**, 024520 (2009), URL <https://link.aps.org/doi/10.1103/PhysRevB.79.024520>.
- ³⁰ R. A. Hein, *Physics Letters* **23**, 435 (1966), ISSN 0031-9163, URL <http://www.sciencedirect.com/science/article/pii/0031916366910808>.
- ³¹ M. P. Mathur, D. W. Deis, C. K. Jones, and W. J. Carr, *Journal of Physics and Chemistry of Solids* **34**, 183 (1973), ISSN 0022-3697, URL <http://www.sciencedirect.com/science/article/pii/0022369773900759>.
- ³² R. D. Zhong, J. A. Schneeloch, X. Y. Shi, Z. J. Xu, C. Zhang, J. M. Tranquada, Q. Li, and G. D. Gu, *Phys. Rev. B* **88**, 020505 (2013), URL <https://link.aps.org/doi/10.1103/PhysRevB.88.020505>.
- ³³ G. Balakrishnan, L. Bawden, S. Cavendish, and M. R. Lees, *Phys. Rev. B* **87**, 140507 (2013), URL <https://link.aps.org/doi/10.1103/PhysRevB.87.140507>.
- ³⁴ N. Haldolaarachchige, Q. Gibson, W. Xie, M. B. Nielsen, S. Kushwaha, and R. J. Cava, *Phys. Rev. B* **93**, 024520 (2016), URL <https://link.aps.org/doi/10.1103/PhysRevB.93.024520>.
- ³⁵ V. Kozii and L. Fu, *Phys. Rev. Lett.* **115**, 207002 (2015), URL <https://link.aps.org/doi/10.1103/PhysRevLett.115.207002>.
- ³⁶ F. Wu and I. Martin, *Phys. Rev. B* **96**, 144504 (2017), URL <https://link.aps.org/doi/10.1103/PhysRevB.96.144504>.
- ³⁷ R. Balian and N. R. Werthamer, *Phys. Rev.* **131**, 1553 (1963), URL <https://link.aps.org/doi/10.1103/PhysRev.131.1553>.
- ³⁸ Y. Tanaka, Z. Ren, T. Sato, K. Nakayama, S. Souma, T. Takahashi, K. Segawa, and Y. Ando, *Nature Physics* **8**, 800 (2012), URL <http://dx.doi.org/10.1038/nphys2442>.
- ³⁹ R. Prozorov and R. W. Giannetta, *Superconductor Science and Technology* **19**, R41 (2006), ISSN 0953-2048, URL <http://stacks.iop.org/0953-2048/19/i=8/a=R01>.
- ⁴⁰ R. Prozorov and V. G. Kogan, *Reports on Progress in Physics* **74**, 124505 (2011), ISSN 0034-4885, URL <http://stacks.iop.org/0034-4885/74/i=12/a=124505>.
- ⁴¹ B. Shen, M. Leroux, Y. L. Wang, X. Luo, V. K. Vlasko-Vlasov, A. E. Koshelev, Z. L. Xiao, U. Welp, W. K. Kwok, M. P. Smylie, et al., *Phys. Rev. B* **91**, 174512 (2015), URL <https://link.aps.org/doi/10.1103/PhysRevB.91.174512>.
- ⁴² M. P. Smylie, M. Leroux, V. Mishra, L. Fang, K. M. Taddei, O. Chmaissem, H. Claus, A. Kayani, A. Snezhko, U. Welp, et al., *Phys. Rev. B* **93**, 115119 (2016), URL <https://link.aps.org/doi/10.1103/PhysRevB.93.115119>.
- ⁴³ M. R. Eskildsen, E. De Waard, C. Dewhurst, S. Kuhn, W. Morgenlander, J. Saroni, and J. White, *Institut Laue-Langevin (ILL)* (2015), URL <https://doi.org/10.5291/ILL-DATA.5-42-388>.
- ⁴⁴ M. A. Kirk and Y. Yan, *Micron* **30**, 507 (1999), ISSN 0968-4328, URL <http://www.sciencedirect.com/science/article/pii/S0968432899000517>.
- ⁴⁵ L. Fang, Y. Jia, J. A. Schlueter, A. Kayani, Z. L. Xiao, H. Claus, U. Welp, A. E. Koshelev, G. W. Crabtree, and W.-K. Kwok, *Phys. Rev. B* **84**, 140504 (2011), URL <https://link.aps.org/doi/10.1103/PhysRevB.84.140504>.
- ⁴⁶ L. Civale, A. D. Marwick, M. W. McElfresh, T. K. Worthington, A. P. Malozemoff, F. H. Holtzberg, J. R. Thompson, and M. A. Kirk, *Phys. Rev. Lett.* **65**, 1164 (1990), URL <https://link.aps.org/doi/10.1103/PhysRevLett.65.1164>.
- ⁴⁷ E. H. Brandt, G. P. Mikitik, and E. Zeldov, *Journal of Experimental and Theoretical Physics* **117**, 439 (2013), ISSN 1090-6509, URL <https://doi.org/10.1134/S1063776113110010>.
- ⁴⁸ A. M. Nikitin, Y. Pan, Y. K. Huang, T. Naka, and A. de Visser, *Phys. Rev. B* **94**, 144516 (2016), URL <https://link.aps.org/doi/10.1103/PhysRevB.94.144516>.
- ⁴⁹ M. Saghir, J. A. T. Barker, G. Balakrishnan, A. D. Hillier, and M. R. Lees, *Phys. Rev. B* **90**, 064508 (2014), URL <https://link.aps.org/doi/10.1103/PhysRevB.90.064508>.
- ⁵⁰ M. R. Eskildsen, *Frontiers of Physics* **6**, 398 (2011), ISSN 1673-3606, URL <https://doi.org/10.1007/s11467-011-0214-z>.
- ⁵¹ F. Gross, B. S. Chandrasekhar, D. Einzel, K. Andres, P. J. Hirschfeld, H. R. Ott, J. Beuers, Z. Fisk, and J. L. Smith, *Zeitschrift für Physik B Condensed Matter* **64**, 175 (1986), ISSN 1431-584X, URL <https://doi.org/10.1007/BF01303700>.
- ⁵² V. K. Maurya, Shruti, P. Srivastava, and S. Patnaik, *EPL (Europhysics Letters)* **108**, 37010 (2014), ISSN 0295-5075, URL <http://stacks.iop.org/0295-5075/108/i=3/a=37010>.
- ⁵³ F. Manzano, A. Carrington, N. E. Hussey, S. Lee, A. Yamamoto, and S. Tajima, *Phys. Rev. Lett.* **88**, 047002 (2002).
- ⁵⁴ J. D. Fletcher, A. Carrington, P. Diener, P. Rodière, J. P. Brison, R. Prozorov, T. Olheiser, and R. W. Giannetta, *Phys. Rev. Lett.* **98**, 057003 (2007), URL <https://link.aps.org/doi/10.1103/PhysRevLett.98.057003>.
- ⁵⁵ F. Marsiglio and J. P. Carbotte, *The Physics of Superconductors, Vol. 1*, p. 223 (Springer Verlag, Berlin, 2003).
- ⁵⁶ L. Fu and E. Berg, *Phys. Rev. Lett.* **105**, 097001 (2010), URL <https://link.aps.org/doi/10.1103/PhysRevLett.105.097001>.
- ⁵⁷ K. Matano, M. Kriener, K. Segawa, Y. Ando, and G.-q. Zheng, *Nat. Phys.* **12**, 852 (2016), ISSN 1745-2473, URL <http://dx.doi.org/10.1038/nphys3781>.
- ⁵⁸ Y. Pan, A. M. Nikitin, G. K. Arazi, Y. K. Huang, Y. Matsushita, T. Naka, and A. de Visser, *Sci. Rep.* **6**, 28632 (2016), URL <http://dx.doi.org/10.1038/srep28632>.
- ⁵⁹ T. Asaba, B. J. Lawson, C. Tinsman, L. Chen, P. Corbae, G. Li, Y. Qiu, Y. S. Hor, L. Fu, and L. Li, *Phys. Rev. X* **7**, 011009 (2017), URL <https://link.aps.org/doi/10.1103/PhysRevX.7.011009>.
- ⁶⁰ P. W. Anderson, *Journal of Physics and Chemistry of Solids* **11**, 26 (1959), ISSN 0022-3697, URL <http://www.sciencedirect.com/science/article/pii/0022369759900368>.
- ⁶¹ K. Michaeli and L. Fu, *Phys. Rev. Lett.* **109**, 187003 (2012), URL <https://link.aps.org/doi/10.1103/PhysRevLett.109.187003>.
- ⁶² Y. Nagai, *Phys. Rev. B* **91**, 060502 (2015), URL <https://link.aps.org/doi/10.1103/PhysRevB.91.060502>.
- ⁶³ M. P. Smylie, K. Willa, H. Claus, A. Snezhko, I. Martin, W.-K. Kwok, Y. Qiu, Y. S. Hor, E. Bokari, P. Niraula, et al., *Phys. Rev. B* **96**, 115145 (2017), URL <https://link.aps.org/doi/10.1103/PhysRevB.96.115145>.
- ⁶⁴ A. A. Abrikosov and L. P. Gor'kov, *Zh. Eksp. Teor. Fiz.* **39** (1960), [*Sov. Phys. JETP* **12**, 1243 (1961)].
- ⁶⁵ L. A. Openov, *Phys. Rev. B* **58**, 9468 (1998), URL <https://link.aps.org/doi/10.1103/PhysRevB.58.9468>.

⁶⁶ I. Martin and P. Phillips, Phys. Rev. B **56**, 14650 (1997), URL <https://link.aps.org/doi/10.1103/PhysRevB.56.14650>.

⁶⁷ H. Mutka, Phys. Rev. B **28**, 2855 (1983), URL <https://link.aps.org/doi/10.1103/PhysRevB.28.2855>.